BIOCHEMISTRY
including biophysical chemistry & molecular biology

Article

pubs.acs.org/biochemistry

A Diferrous-Dinitrosyl Intermediate in the N_2O-Generating Pathway of a Deflavinated Flavo-Diiron Protein

Jonathan D. Caranto,[†] Andrew Weitz,[‡] Nitai Giri,[†] Michael P. Hendrich,*[,‡] and Donald M. Kurtz, Jr.*[,†]

[†]Department of Chemistry, University of Texas at San Antonio, San Antonio, Texas 78249, United States

[‡]Department of Chemistry, Carnegie Mellon University, Pittsburgh, Pennsylvania 15213, United States

Supporting Information

ABSTRACT: Flavo-diiron proteins (FDPs) function as anaerobic nitric oxide scavengers in some microorganisms, catalyzing reduction of nitric to nitrous oxide. The FDP from *Thermotoga maritima* can be prepared in a deflavinated form with an intact diferric site (deflavo-FDP). Hayashi et al. [(2010) *Biochemistry 49*, 7040−7049] reported that reaction of NO with reduced deflavo-FDP produced substoichiometric N_2O. Here we report a multispectroscopic approach to identify the iron species in the reactions of deflavo-FDP with NO. Mössbauer spectroscopy identified two distinct ferrous species after reduction of the antiferromagnetically coupled diferric site. Approximately 60% of the total ferrous iron was assigned to a diferrous species associated with the N_2O-generating pathway. This pathway proceeds through successive diferrous-mononitrosyl ($S = {}^1/_2$ $Fe^{II}\{FeNO\}^7$) and diferrous-dinitrosyl ($S = 0$ $[\{FeNO\}^7]_2$) species that form within ∼100 ms of mixing of the reduced protein with NO. The diferrous-dinitrosyl intermediate converted to an antiferromagnetically coupled diferric species that was spectroscopically indistinguishable from that in the starting deflavinated protein. These diiron species closely resembled those reported for the flavinated FDP [Caranto et al. (2014) *J. Am. Chem. Soc. 136*, 7981−7992], and the time scales of their formation and decay were consistent with the steady state turnover of the flavinated protein. The remaining ∼40% of ferrous iron was inactive in N_2O generation but reversibly bound NO to give an $S = {}^3/_2$ $\{FeNO\}^7$ species. The results demonstrate that N_2O formation in FDPs can occur via conversion of $S = 0$ $[\{FeNO\}^7]_2$ to a diferric form without participation of the flavin cofactor.

Flavo-diiron proteins (FDPs) are soluble cytoplasmic enzymes that catalyze reductive scavenging of dioxygen and/or nitric oxide in anaerobic or microaerophilic microorganisms.[1−10] The active sites of FDPs contain a unique combination of nonheme diiron-carboxylate and flavin mononucleotide (FMN) cofactors, as shown in Scheme 1.

Scheme 1

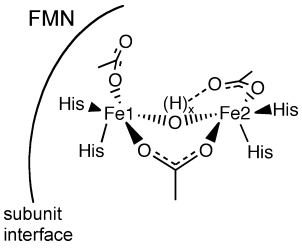

FDPs function as the terminal component in catalysis of reduction of nitric oxide to nitrous oxide using NADH as the source of reducing equivalents in a process termed nitric oxide reductase (NOR) activity. The nitric oxide reduction occurs at the fully reduced FDP active site ($FMNH_2$-$Fe^{II}Fe^{II}$), which can reduce up to four molecules of NO to two molecules of N_2O, leading to the fully oxidized (FMN-$Fe^{III}Fe^{III}$) active site. To separate the roles of the FMN and diiron sites in NOR turnover, a deflavinated FDP (deflavo-FDP) from *Thermotoga maritima* (Tm) was investigated. The X-ray crystal structure of Tm deflavo-FDP (Protein Data Bank entry 1VME) retained the head-to-tail homodimeric subunit arrangement and diiron site structure characteristic of flavinated FDPs.[11,12] The dithionite-reduced deflavo-FDP reacted with ≤1 equiv of NO to form a stable antiferromagnetically coupled diferrous-mononitrosyl species ($Fe^{II}\{FeNO\}^7$) with ground spin state $S = {}^1/_2$ due to antiferromagnetic coupling between the $S = 2$ Fe^{II} and $S = {}^3/_2$ $\{FeNO\}^7$ centers[11] ($\{FeNO\}^7$ is the Enemark−Feltham notation for ferrous-nitrosyl[13]). This through-bond coupling requires retention of at least one of the bridging iron ligands shown in Scheme 1.[14,15] Reaction of the reduced deflavo-FDP with excess NO led to substoichiometric (with respect to diiron sites) generation of N_2O and a stable $S = {}^3/_2$ $\{FeNO\}^7$ species.[11] These reactions were proposed to occur as illustrated in Scheme 2 (where the curved line underneath the iron pairs represents bridging ligand(s) from the protein and/or solvent). The putative antiferromagnetically coupled diferric product of the N_2O-generating pathway was inferred from the absence of any other iron-associated EPR signals and the UV−vis absorption difference spectra of the NO-reacted protein.[11] The stable $S = {}^3/_2$ $\{FeNO\}^7$ species in the NO-reacted protein was proposed to arise from a portion of the diferrous-

Received: July 7, 2014
Revised: August 20, 2014
Published: August 21, 2014

   dx.doi.org/10.1021/bi500836z | *Biochemistry* 2014, 53, 5631−5637

Scheme 2

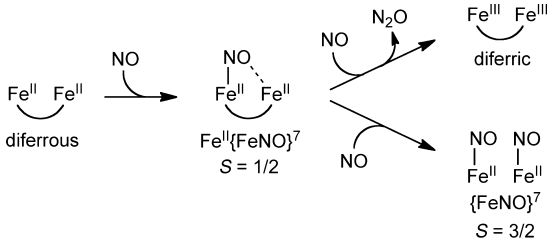

mononitrosyl sites in which the iron centers became magnetically uncoupled upon addition of the second NO, presumably as a consequence of loss of the bridging ligand(s). A stable diferrous-mononitrosyl ($S = {}^1/_2$ $Fe^{II}\{FeNO\}^7$) species was also generated upon reaction of the fully reduced flavinated FDP ($FMNH_2$-$Fe^{II}Fe^{II}$) active site with ≤1 equiv of NO.[16]

We have more recently reported that reaction of the fully reduced flavinated FDP with excess NO led to an antiferromagnetically coupled diferrous-dinitrosyl ($S = 0$ $[\{FeNO\}^7]_2$) intermediate preceding $FMNH_2$ oxidation and formation of diferric sites.[17] On the basis of those results, we suggested that the $S = 0$ $[\{FeNO\}^7]_2$ could convert to $S = 0$ $Fe^{III}Fe^{III}$ (diferric) and N_2O without redox participation of the flavin cofactor. Mössbauer spectroscopy was crucial to identification of these various iron species. Here we report an analogous multispectroscopic approach to characterization of intermediates and products in the deflavo-FDP reactions with NO. Our results indicate that the apparent branching shown in Scheme 2 originates from two distinguishable types of ferrous sites and not from two differing reactions of the $S = {}^1/_2$ diferrous-mononitrosyl species. Together with the previous reports,[11,17] our deflavo-FDP results confirm that N_2O formation can occur via conversion of an $S = 0$ $[\{FeNO\}^7]_2$ intermediate to $S = 0$ diferric and clearly demonstrate that this conversion can occur without the flavin cofactor. All results reported here were obtained on the Tm deflavo-FDP.

MATERIALS AND METHODS

Reagents and General Procedures. Reagents and buffers were of the highest grade commercially available. All reagents, protein, and media solutions were prepared using water that had been passed through a Milli-Q ultrapurification system (Merck Millipore, Inc.) to achieve a resistivity of 18 MΩ. The buffer used for all experiments was 50 mM 3-(*N*-morpholino)-propanesulfonic acid (MOPS) (pH 7.3), which is hereafter termed buffer. Expression, isolation, and purification of Tm FDP[12] and ^{57}Fe-enriched Tm FDP,[17] analyses of protein, iron, and FMN,[12] and preparation and calibration of ∼1.8 mM nitric oxide aqueous stock solutions from gaseous NO or ∼20 mM NO delivery equivalent stock solutions of disodium 1-[(2-carboxylato)pyrrolidin-1-yl]diazen-1-ium 1,2-diolate (PROLI-NONOate) (Cayman Chemical Co.)[17] were conducted as described in the cited references. The as-isolated Tm FDP routinely contained ∼2 Fe and ≤0.2 FMN per monomer for both natural isotopic abundance and ^{57}Fe-enriched proteins. The residual FMN was removed by the previously described protocol.[11] All deflavo-FDP samples used in this work were analyzed to contain ∼2 Fe/protein monomer. Deflavo-FDP concentrations were determined using an ε_{280} of 110000 M^{-1} cm^{-1} (previously determined using the bicinchonic acid protein assay). All FDP concentrations are given in protein monomer, i.e., in diiron site equivalents. Reduced deflavo-FDP was prepared by addition of 1 molar equiv of sodium dithionite from a concentrated stock solution to anaerobic as-isolated deflavo-FDP solutions in buffer followed by incubation for ∼1 h at room temperature.

Manually Mixed Mössbauer Spectral Samples of Reduced Deflavo-FDP with Substoichiometric NO. All manipulations were conducted in an anaerobic N_2-filled glovebox equipped with a liquid N_2-cooled cold well (Vacuum Atmospheres Co.). The samples were prepared at room temperature from 800 μL of a 500 μM ^{57}Fe-enriched reduced deflavo-FDP solution; 400 μL of this solution was pipetted into a Mössbauer cup and frozen in the cold well. To the remaining 400 μL was added 8 μL of a PROLI-NONOate stock solution in deoxygenated 10 mM NaOH containing 20 mM NO delivery equivalents. The protein/PROLI-NONOate mixture was incubated for 5 min, then pipetted into a Mössbauer cup, and frozen in the cold well. The frozen samples were removed from the glovebox and stored at 77 K until data were collected.

Rapid Kinetics. Stopped-flow UV−vis absorption spectrophotometry and RFQ spectral sample preparations were performed essentially as described previously for the flavinated Tm FDP.[17] More detailed descriptions of these procedures for the deflavo-FDP are provided in the Supporting Information.

Spectroscopies. EPR spectra were recorded on a Bruker ESP 300E X-band spectrometer equipped with a model ESR 900 (Oxford Instruments, Inc.) helium continuous-flow cryostat. The following standard parameters were used for spectral collection: modulation frequency, 100 kHz; modulation amplitude, 10.5 G; conversion time, 81.92 ms; time constant, 5.12 ms. The microwave power and temperature were adjusted to collect spectra under nonsaturating conditions, and these values are listed in the figure captions. ^{57}Fe Mössbauer spectra were recorded with two spectrometers using a Janis Research Super-Varitemp dewar. Isomer shifts are reported relative to Fe metal at 298 K. The simulations of Mössbauer spectra were calculated with least-squares fitting using SpinCount and the standard spin Hamiltonian described previously.[17]

RESULTS AND DISCUSSION

Two Spectroscopically Distinct Iron Sites in Reduced Deflavo-FDP. The as-isolated deflavo-FDP Mössbauer spectrum (Figure 1A) showed a single doublet with parameters typical of high-spin ferric centers (Table 1). The lack of effect of an applied magnetic field and the single sharp doublet (line width $\Gamma = 0.31$ mm/s) at low temperatures was indicative of an antiferromagnetic exchange interaction between equivalent iron centers to give an $S = 0$ spin state lowest in energy. No EPR or Mössbauer spectroscopic features that could be assigned to mononuclear high-spin ferric sites were apparent. On the basis of the UV−vis absorption spectrum and EPR silence, the anaerobic treatment of as-isolated deflavo-FDP with dithionite was presumed to reduce the antiferromagnetically coupled diferric site to ferrous.[11] The ^{57}Fe Mössbauer spectral data in Figure 1B and Table 1 confirmed that all the iron was indeed reduced to the ferrous state. The Mössbauer spectra of the dithionite-reduced deflavo-FDP showed two doublets having parameters typical of high-spin ferrous (Table 1). The corresponding species comprised 60 and 40% of the total iron and will be termed $diFe^{II}$ and Fe^{II}_i (Figure 1B), respectively. The Mössbauer parameters of $diFe^{II}$ were indistinguishable from those of the diferrous site previously reported for the reduced flavinated FDP ($FMNH_2$-$Fe^{II}Fe^{II}$).[17]

dx.doi.org/10.1021/bi500836z | *Biochemistry* 2014, 53, 5631−5637

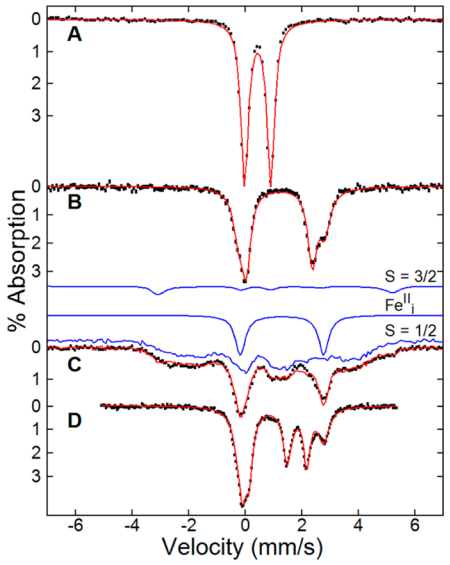

Figure 1. ^{57}Fe Mössbauer spectra of (A) as-isolated deflavo-FDP, (B) reduced deflavo-FDP, and (C and D) reduced deflavo-FDP after addition of 0.8 equiv of NO in buffer. The red traces are simulations of the data (black vertical bars) using the parameters listed in Table 1 for (A) diFe^{III}, (B) 60% diFe^{II} and 40% Fe$^{II}_i$, and (C and D) 60% Fe^{II}{FeNO}^{7}, 30% Fe$^{II}_i$, and 10% $S = {}^3/_2$ {FeNO}^{7}. The blue traces show the components of spectrum C, where the $S = {}^1/_2$ trace is an experimental spectrum of Fe^{II}{FeNO}^{7} in the flavinated FDP.[17] The magnetic parameters for the $S = {}^3/_2$ simulation are as follows: D = 12 cm^{-1}, E/D = 0, and **A** = (−26, −25, −27) T.[17] The spectra were collected at 4.2 K (A−C) or 100 K (D) with a 45 mT magnetic field applied parallel to the γ-ray direction. All spectral samples contained 500 μM diiron site equivalents.

Table 1. Mössbauer Spectral Parameters for Iron Species in Deflavo-FDP and Resulting from Reactions of Reduced Deflavo-FDP with NO

species	δ (mm/s)	ΔE_Q (mm/s)
diFe^{III}	0.44	0.92
diFe^{II}	1.20	2.34
Fe$^{II}_i$	1.28	3.04
Fe^{II}{FeNO}^{7}	1.15	2.05
Fe^{II}{FeNO}^{7}	0.69	1.59
$S = 0$ [{FeNO}^{7}]$_2$	0.74	1.85
$S = {}^3/_2$ {FeNO}^{7}	∼0.65	∼−1.9

The Fe$^{II}_i$ species was not observed in the flavinated FDP, and on the basis of the evidence presented below, we use the subscript "i" to indicate that this species is "inactive" with respect to the N_2O-generating pathway.

Mössbauer Spectroscopy Reveals Differing Reactivities of diFe^{II} and Fe$^{II}_i$ with Substoichiometric NO. The Mössbauer spectrum resulting from manual mixing of reduced deflavo-FDP with substoichiometric NO obtained at 100 K (Figure 1D) exhibited three doublets. The doublet corresponding to diFe^{II} of the unreacted deflavo-FDP was absent. Two of the doublets had equal areas and exhibited Mössbauer parameters indicative of Fe^{II} (δ = 1.15 mm/s, and ΔE_Q = 2.05 mm/s) and {FeNO}^{7} (δ = 0.69 mm/s, and ΔE_Q = 1.59 mm/s) components of the $S = {}^1/_2$ Fe^{II}{FeNO}^{7} species previously observed in the flavinated FDP.[17] The combined area of the Fe^{II}{FeNO}^{7} doublets was within error equal to that of the diFe^{II} species (60%) in the unreacted sample. The third doublet in Figure 1D with δ = 1.28 mm/s and ΔE_Q = 3.04 mm/s was identical to that of Fe$^{II}_i$ in unreacted deflavo-FDP. This Fe$^{II}_i$ species accounted for 30% of the iron in the NO-reacted sample, which was less than the 40% Fe$^{II}_i$ in the unreacted sample. The remaining 10% of total iron in the NO-reacted sample was a magnetically isolated $S = {}^3/_2$ {FeNO}^{7} species ($\delta \sim 0.65$ mm/s, and $\Delta E_Q \sim -1.9$ mm/s), which was observed in the low-temperature spectrum (Figure 1C). Thus, with substoichiometric NO, all of the diFe^{II} reacted to form $S = {}^1/_2$ Fe^{II}{FeNO}^{7}, whereas only a portion of Fe$^{II}_i$ reacted to give an $S = {}^3/_2$ {FeNO}^{7} species. These results imply that diFe^{II} has a higher affinity for NO than does Fe$^{II}_i$. The total percentage of NO-bound iron species, 40% (30% $S = {}^1/_2$ Fe^{II}{FeNO}^{7} plus 10% $S = {}^3/_2$ {FeNO}^{7}), obtained from the Mössbauer spectra was in good agreement with the ∼0.4 equiv of added NO per iron. The manual mixing conditions for the Mössbauer samples (see Materials and Methods) indicated that the {FeNO}^{7} species formed with substoichiometric NO were stable on a time scale of at least minutes. The lack of diferric species also indicated that no turnover occurred with substoichiometric NO on this time scale.

A Stable $S = {}^1/_2$ Diferrous-Mononitrosyl Formed within 100 ms of Mixing Reduced Deflavo-FDP with Substoichiometric NO. Previously reported manual addition of ∼1 equiv of NO to reduced deflavo-FDP resulted in a UV−vis absorption spectral signature for {FeNO}^{7}.[11] The stopped-flow UV−vis absorption spectral time course (Figure 2A) developed the same {FeNO}^{7} spectral signature with features at 420 nm (ε = 1350 M^{-1} cm^{-1}), 459 nm (ε = 1300 M^{-1} cm^{-1}), and 630 nm (ε = 400 M^{-1} cm^{-1}) within ∼60 ms of mixing. The corresponding 300 s time course (Figure 2B) showed that this {FeNO}^{7} spectral species was stable for at least several minutes, which was also consistent with the manually mixed samples.[11] Similarly, the 200 ms RFQ EPR spectrum of reduced deflavo-FDP mixed with substoichiometric NO (∼0.6 NO per two irons) exhibited the expected $S = {}^1/_2$ EPR spectrum of Fe^{II}{FeNO}^{7} (Figure 2C),[11,16] and the spin concentration in the RFQ sample was nearly equal to the concentration of the delivered NO.

Rapid Reactions of Reduced Deflavo-FDP with Excess NO. Stopped-flow UV−vis absorption spectral time courses for reactions of reduced deflavo-FDP with excess NO (Figure 3) showed the formation of two successive {FeNO}^{7} species followed by a decay phase. The initial spectrum at 1.3 ms after the mixing dead time (Figure 3A) exhibited a shoulder at ∼420 nm, which is a characteristic feature in the absorption spectrum of Fe^{II}{FeNO}^{7} (cf. Figure 2).[11] This shoulder became less prominent as the time course approached 130 ms, during which a more intense {FeNO}^{7} absorption spectrum developed. This more intense absorption was maximized at ∼130 ms with features at 340 nm (ε = 3000 M^{-1} cm^{-1}), 453 nm (ε = 2000 M^{-1} cm^{-1}) and 630 nm (ε = 500 M^{-1} cm^{-1}). These features and the 453 nm extinction[11] are consistent with conversion of essentially all the ferrous centers to {FeNO}^{7} within 130 ms. The corresponding stopped-flow reaction monitored over a 300 s time course (Figure 3B) showed gradual but not complete disappearance of the {FeNO}^{7} spectrum. Little or no further decrease in the spectral intensity of Figure 3B was observed beyond 300 s. The 300 s UV−vis absorption spectrum resembles that of manually mixed samples[11] and, as inferred for those samples, likely contains contributions from {FeNO}^{7} and diferric spectra (see below).

dx.doi.org/10.1021/bi500836z | Biochemistry 2014, 53, 5631−5637

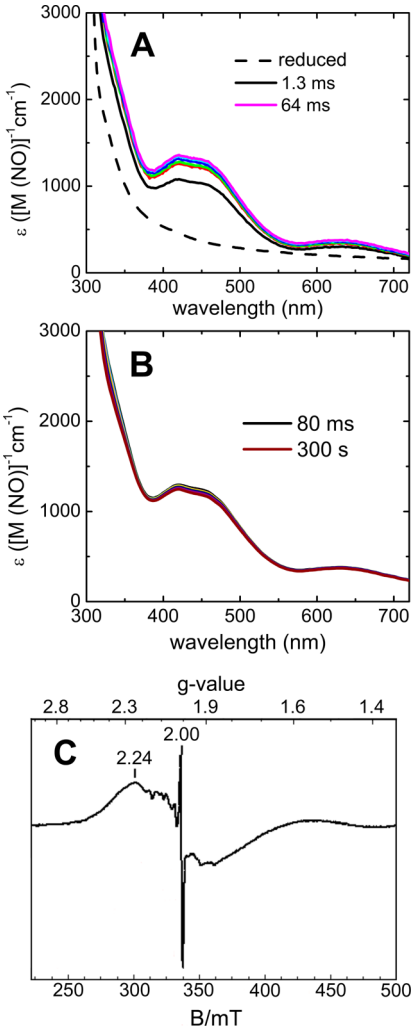

Figure 2. (A) 64 ms and (B) 300 s UV−vis absorption stopped-flow spectral time courses of the reaction of reduced deflavo-FDP with substoichiometric NO at 3 °C. The dashed trace in panel A is the spectrum of the reduced deflavo-FDP stopped-flow mixed with deoxygenated buffer in place of NO-containing buffer. Spectra in panel A were obtained in 13 ms intervals after the initial 1.3 ms spectrum. Concentrations immediately after mixing were 190 μM reduced deflavo-FDP and 155 μM NO. The extinction coefficient axis is based on the delivered NO concentration. (C) RFQ EPR spectra of 950 μM reduced deflavo-FDP mixed with 560 μM NO (concentrations after mixing) in buffer at 4 °C and quenched at 200 ms. The EPR spectrum was collected at 4 K with a microwave power of 2.1 mW. The $S = {}^1/_2$ species was at a concentration of 520 μM as determined by double integration against a Cu^{II}(EDTA) standard.[17] The sharp $g = 2$ signal is due to a very small amount of an organic radical, possibly residual FMN semiquinone. The minor sharp features straddling $g = 2$ are due to a Mn(II) impurity.

Corresponding RFQ EPR spectra for the reaction of reduced deflavo-FDP with excess NO collected at quench times of 130 ms, 10 s, and 60 s are shown in Figure 4. The $S = {}^1/_2$ Fe^{II}{FeNO}^{7} signal was absent in all of these spectra. The signal with g values at 4.16 and 3.90 is due to an $S = {}^3/_2$ {FeNO}^{7} species, which formed within 100 ms after mixing and did not change in intensity over at least 60 s. The average of the $S = {}^3/_2$ spin concentrations in the RFQ EPR samples was approximately 1 per diiron site, indicating approximately half the iron consisted of magnetically isolated {FeNO}^{7} centers, and that these centers formed within 130 ms of mixing with

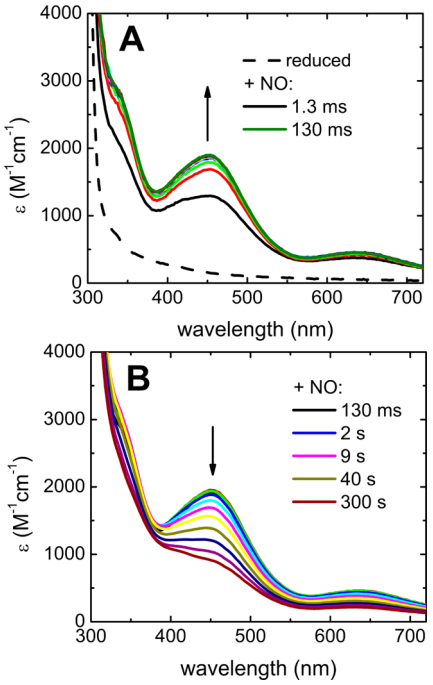

Figure 3. (A) 130 ms and (B) 300 s stopped-flow UV−vis absorption spectral time courses for reactions of reduced deflavo-FDP with excess NO at 4 °C. The dashed trace in panel A is the spectrum resulting from stopped-flow mixing of reduced deflavo-FDP with deoxygenated buffer in place of NO-saturated buffer. Subsequent spectra are shown in 13 ms increments up to 130 ms. The spectra in panel B were collected on a logarithmic time scale from 130 ms to 300 s. Concentrations immediately after mixing were 180 μM reduced deflavo-FDP and 900 μM NO in buffer. The extinction coefficient axis is based on diiron site concentration. Arrows indicate directions of absorbance changes. This figure was reproduced from the Supporting Information of ref 17. Copyright 2014 American Chemical Society.

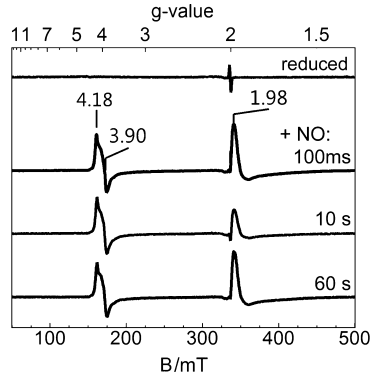

Figure 4. RFQ EPR spectral time course of the reaction of reduced deflavo-FDP with excess NO in buffer at 2 °C. Spectra were recorded at 4 K and a microwave power of 260 μW. The reduced spectrum was obtained prior to mixing with NO. Quench times following mixing with NO are indicated in the figure. Concentrations immediately after mixing were 120 μM diiron site equivalents and 1500 μM NO. The $g = 1.98$ signal in these spectra is due to the excess NO in the samples. $S = {}^3/_2$ spins were quantified by comparison to an Fe^{II}(EDTA)NO standard.[17]

excess NO. Because the stopped-flow UV−vis absorption spectral time course with excess NO (Figure 3A) showed that essentially all the iron formed {FeNO}^{7} within 130 ms, approximately half the {FeNO}^{7} in the RFQ samples of Figure

dx.doi.org/10.1021/bi500836z | Biochemistry 2014, 53, 5631−5637

4 must be EPR silent at a reaction time of ~100 ms. It can be further inferred that the residual {FeNO}^{7} UV−vis absorption at 300 s in Figure 3B corresponds to the constant-intensity $S = {}^3/_2$ {FeNO}^{7} EPR signal in Figure 4. This in turn implies that the EPR silent ~50% of the rapidly formed {FeNO}^{7} decayed to another EPR silent species with much lower UV−vis absorption over the course of a few minutes. Anticipating the Mössbauer results described below, we associate these two EPR silent species with the diferrous-dinitrosyl and diferric species of the N_2O-generating pathway shown in Scheme 3.

Scheme 3

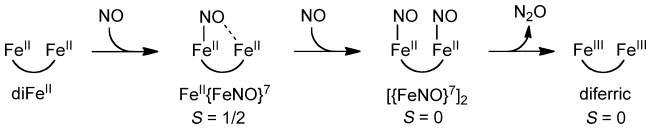

RFQ Mössbauer Associates diFe^{II} with the N_2O-Generating Pathway. RFQ Mössbauer and parallel EPR spectra of reduced deflavo-FDP mixed with 3 equiv of NO (the highest practicable molar ratio that can be achieved in our system[17]) were collected at quench times of 100 ms and 60 s. The RFQ Mössbauer spectra are shown in Figure 5, and the

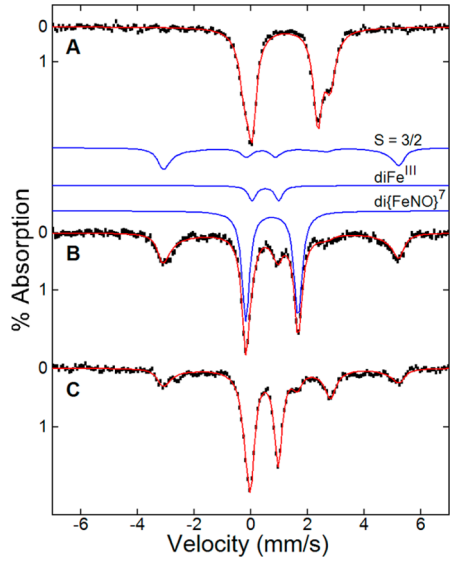

Figure 5. RFQ Mössbauer spectra of (A) reduced deflavo-FDP and reduced deflavo-FDP mixed with 3 equiv of NO per diiron site in buffer and quenched at (B) 100 ms or (C) 60 s. The red traces are simulations of the data (black vertical bars) using the parameters and the percent iron compositions listed in Tables 1 and 2, respectively. The blue traces show the components of spectrum B. The $S = {}^3/_2$ magnetic parameters are given in the legend of Figure 1. The spectra were collected at 4.2 K and a magnetic field of 45 mT applied parallel to the γ-ray direction. Concentrations immediately after mixing were 500 μM reduced deflavo-FDP and 1500 μM NO.

percentages of total iron for the various species are listed in Table 2. At a reaction time of 100 ms, the diFe^{II} and Fe$^{II}_i$ spectral features of the reduced deflavo FDP were replaced by three new spectral species. Two of these species were doublets at 4 K, indicative of either diamagnetic or integer spin systems. The parameters of the most prominent doublet at 100 ms (δ = 0.74 mm/s, and ΔE_Q = 1.85 mm/s) were nearly identical to those assigned to the antiferromagnetically coupled

Table 2. Percentages of Total Iron for the ^{57}Fe Mössbauer Spectral Species of Reduced Deflavo-FDP and after RFQ Reactions with 3 equiv of NO per Diiron Site[a]

reaction time	diFe^{II}	[{FeNO}^{7}]$_2$	diFe^{III}	Fe$^{II}_i$	$S = {}^3/_2$ {FeNO}^{7}
0 s[b]	63	0	0	37	0
100 ms	0	55	7	0	38
60 s	0	10	47	23	20

[a]From the spectra in Figure 5. [b]In the absence of NO from Figure 1.

[{FeNO}^{7}]$_2$ intermediate along the NOR catalytic pathway recently reported for the flavinated FDP.[17] Therefore, this doublet in Figure 5 was assigned to the S = 0 [{FeNO}^{7}]$_2$ intermediate along the N_2O-generating pathway in Scheme 3. The second doublet in the 100 ms spectrum (diFe^{III} in Table 2) has spectral parameters identical to those of the antiferromagnetically coupled diferric site in as-isolated deflavo-FDP (Figure 1A and Table 1). Because this doublet did not appear in the spectrum of the starting reduced deflavo-FDP, it was assigned to the diferric product of the N_2O-generating pathway in Scheme 3. The Mössbauer spectral species assigned to S = 0 [{FeNO}^{7}]$_2$ and diferric sites at 100 ms (Figure 5B and Table 2) together accounted for 62% of the total iron, which was equal to that of diFe^{II} prior to reaction with NO. Between 100 ms and 60 s, the S = 0 [{FeNO}^{7}]$_2$ spectral species decreased from 55 to 10% of the iron sites, and the diFe^{III} species increased from 7 to 47% percent of the total iron. Here again, the total of these two species, 57%, was approximately the same as that of diFe^{II} prior to reaction with NO. The diFe^{II}, S = 0 [{FeNO}^{7}]$_2$, and diFe^{III} species are thus logically assigned to the N_2O-generating pathway in Scheme 3.

The third spectral component, labeled $S = {}^3/_2$ in the 100 ms spectrum of Figure 5, exhibited hyperfine splitting at 4 K and is characteristic of magnetically isolated $S = {}^3/_2$ {FeNO}^{7}.[18] The percentage of the spectral species assigned to $S = {}^3/_2$ {FeNO}^{7} in the 100 ms RFQ Mössbauer spectrum (Figure 5B) was equal to that of Fe$^{II}_i$ prior to reaction with NO (Table 2). This observation is consistent with assignment of $S = {}^3/_2$ {FeNO}^{7} as the reaction product of Fe$^{II}_i$ in the presence of excess NO, as was the case with substoichiometric NO. No $S = {}^1/_2$ Fe^{II}{FeNO}^{7} spectral components were present in any of these RFQ Mössbauer spectra (or in the parallel RFQ EPR spectra shown in Figure 6).

Between 100 ms and 60 s, the RFQ Mössbauer spectral species assigned to $S = {}^3/_2$ {FeNO}^{7} decreased from 38 to 20% in a manner concomitant with the reappearance of the Fe$^{II}_i$ species (Table 2). EPR spectra of these RFQ Mössbauer samples (Figure 6) showed a parallel decrease in the magnitude of the $S = {}^3/_2$ signal. This observation would seem to be inconsistent with the RFQ EPR time course in Figure 4, which showed no such decrease in the magnitude of the $S = {}^3/_2$ signal. Unlike the time course in Figure 4, Figure 6 shows that the g = 1.98 signal due to free NO had disappeared in the 60 s spectrum. Because the RFQ Mössbauer samples and their corresponding EPR samples contained 1 mM total iron, a maximum of 1 mM of the initial 1.5 mM NO could have been consumed by reaction with the FDP (assuming 1 mol of NO reaction/mol of iron). This stoichiometry was consistent with the 100 ms RFQ Mössbauer spectrum, which showed that all of the iron is in the form of either {FeNO}^{7} or diferric species. The disappearance of the free NO signal in the 60 s EPR spectrum in Figure 6 could be due to escape of NO from either the drive syringe or the mixing circuit in the interim between

dx.doi.org/10.1021/bi500836z | Biochemistry 2014, 53, 5631−5637

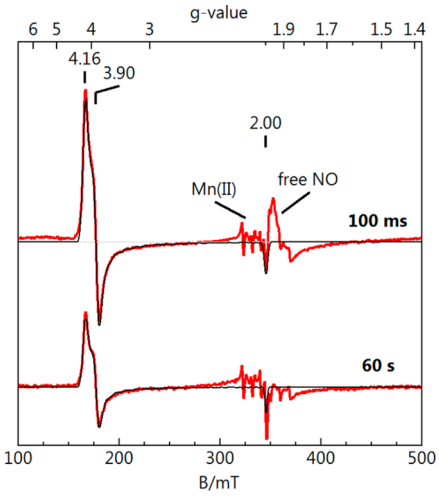

Figure 6. RFQ EPR spectra of reduced deflavo-FDP mixed with 3 equiv of NO in buffer and quenched at 100 ms and 60 s. The spectra were obtained on portions of the same quenched samples used for the Mössbauer spectra shown in Figure 5. The EPR spectra were collected at 11 K and a microwave power of 200 μW. Concentrations immediately after mixing were 500 μM reduced deflavo-FDP and 1500 μM NO. The sharp features straddling $g = 2$ are due to a Mn(II) impurity. The simulations (black lines) are for an $S = {}^3/_2$ species with $E/D = 0.021$. The $S = {}^3/_2$ spin concentrations were determined with the software SpinCount developed by M. P. Hendrich.

collection of the 100 ms and 60 s samples. In any case, the decrease in the level of the $S = {}^3/_2$ {FeNO}^{7} species and reappearance of Fe^{II}_i in the 60 s sample can be attributed to dissociation of NO from the $S = {}^3/_2$ {FeNO}^{7} species accompanying the loss of free NO. This observation is consistent with the apparently lower affinity of NO for Fe^{II}_i compared to that of diFe^{II} observed in the reactions with substoichiometric NO (Figure 1). The absence of diFe^{II} in the 60 s RFQ Mössbauer spectrum (Table 2) is consistent with the turnover of diFe^{II} according to Scheme 3. The reappearance of Fe^{II}_i at 60 s indicates its reaction with NO is limited to reversible formation of {FeNO}^{7}.

Upon exposure of the 60 s RFQ Mössbauer sample to air by passing the sample in and out of a pipet for 5 min, the resulting spectrum (Figure S1 of the Supporting Information) showed two species: diFe^{III} (69%) and Fe^{II}_i (23%). The amount of diFe^{III} was approximately equal to the amount of the diFe^{II} species before the addition of NO. The percentage of Fe^{II}_i species was unchanged, indicating that it was not oxidized under these conditions. This air-exposed sample was transferred to an EPR tube and frozen in liquid N_2. A mononuclear $S = {}^5/_2$ Fe^{III} EPR signal (not shown) was detected at 26 K and determined to account for 8% of the iron, an amount that was within the noise of the Mössbauer spectrum. No $S = {}^3/_2$ EPR signal was detected in this air-exposed sample.

N_2O-Generating Pathway in FDP. The combined spectroscopic and rapid kinetics results indicate that the N_2O-generating pathway in deflavo-FDP is that shown in Scheme 3, which originates from the species identified here as diFe^{II}. This species accounted for 60% of total iron, which is consistent with previously reported yields of N_2O from reactions of reduced deflavo-FDP with excess NO.[11] Our Mössbauer results verify the ultimate production of antiferromagnetically coupled diferric sites (diFe^{III}) quantitatively upon reaction of the diFe^{II} species with excess NO. These NO-generated diferric sites are spectroscopically indistinguishable from those in the as-isolated FDP. We have no direct spectroscopic evidence of bridging ligand(s) in the diFe^{II} species. However, because all the other species in Scheme 3 must contain bridging ligands to mediate their antiferromagnetic coupling, retention of at least one of the bridging ligands shown in Scheme 1 would seem to be a reasonable presumption for diFe^{II}.

Our results associate the $S = {}^3/_2$ {FeNO}^{7} species in the deflavo-FDP with an inactive ferrous species (Fe^{II}_i), which was not detected in the flavinated FDP.[17] In the as-isolated deflavo-FDP, we observed only one population of iron, consisting of antiferromagnetically coupled diferric sites ($S_{Tot} = 0$). Similarly, the crystal structure of our preparation of the as-isolated deflavo-FDP showed intact diiron sites having the structure depicted in Scheme 1 in both subunits of the homodimer.[11] The minority population of Fe^{II}_i sites must, therefore, have been generated during or after reduction of the as-isolated deflavinated protein.

All of the species along the N_2O-generating pathway shown in Scheme 3 for the deflavo-FDP had spectroscopic parameters and kinetic behaviors very close to or indistinguishable from their counterparts in the flavinated FDP.[17] As was the case for the flavinated protein, only one sharp Mössbauer doublet was observed for the diferrous-dinitrosyl ($S = 0$ [{FeNO}^{7}]$_2$) species in the deflavo-FDP, consistent with very similar coordination spheres for the individual {FeNO}^{7} centers. Despite these nearly identical Mössbauer parameters, the diFe^{II} site of the deflavo-FDP appeared to have a significantly higher affinity for the second NO compared to that of the diferrous site in the flavinated FDP. This higher second NO affinity of the diFe^{II} site in the deflavo-FDP was inferred from the absence of the diferrous-mononitrosyl and presence of the diferrous-dinitrosyl species at 100 ms in the RFQ reaction with excess NO (Figure 4 and Table 2). The RFQ reaction of reduced flavinated FDP with the same excess of NO, on the other hand, showed a substantial amount of the diferrous-mononitrosyl species along with the diferrous-dinitrosyl species in the 100–200 ms time range (which preceded any significant $FMNH_2$ oxidation).[17] How the absence of the FMN cofactor could lead to this increased second NO affinity of the diFe^{II} site in the deflavo-FDP is not obvious, given the close resemblance of the protein and diiron site structures in the Tm deflavo-FDP to those of other flavinated FDPs.[3,12,19] In any case, our results confirm that catalytically competent N_2O generation in FDP can occur via conversion of an antiferromagnetically coupled [{FeNO}^{7}]$_2$ site to a diferric site and that the FMN cofactor is not required for this conversion.

■ ASSOCIATED CONTENT

Supporting Information

Experimental details and Mössbauer spectrum of air-exposed sample. This material is available free of charge via the Internet at http://pubs.acs.org.

■ AUTHOR INFORMATION

Corresponding Authors

*E-mail: donald.kurtz@utsa.edu.
*E-mail: hendrich@andrew.cmu.edu.

Funding

This work was supported by National Institutes of Health Grants GM040388 to D.M.K., GM077387 to M.P.H., and MBRS/RISE GM060655 to J.D.C.

Notes

The authors declare no competing financial interest.

■ ABBREVIATIONS

FDP, flavodiiron proteins; NOR, nitric oxide reductase; Tm, *T. maritima*; MOPS, 3-(*N*-morpholino)propanesulfonic acid; PROLI-NONOate, disodium 1-[(2-carboxylato)pyrrolidin-1-yl]diazen-1-ium 1,2-diolate; EDTA, ethylenediaminetetraacetic acid; RFQ, rapid freeze quench.

■ REFERENCES

(1) Saraiva, L. M., Vicente, J. B., and Teixeira, M. (2004) The role of the flavodiiron proteins in microbial nitric oxide detoxification. *Adv. Microb. Physiol. 49*, 77−129.

(2) Vine, C. E., and Cole, J. A. (2011) Unresolved sources, sinks, and pathways for the recovery of enteric bacteria from nitrosative stress. *FEMS Microbiol. Lett. 325*, 99−107.

(3) Kurtz, D. M., Jr. (2007) Flavo-diiron enzymes: Nitric oxide or dioxygen reductases? *Dalton Trans.*, 4115−4121.

(4) Rodrigues, R., Vicente, J. B., Felix, R., Oliveira, S., Teixeira, M., and Rodrigues-Pousada, C. (2006) *Desulfovibrio gigas* flavodiiron protein affords protection against nitrosative stress in vivo. *J. Bacteriol. 188*, 2745−2751.

(5) Vicente, J. B., Tran, V., Pinto, L., Teixeira, M., and Singh, U. (2012) A detoxifying oxygen reductase in the anaerobic protozoan *Entamoeba histolytica*. *Eukaryotic Cell 11*, 1112−1118.

(6) Mills, P. C., Rowley, G., Spiro, S., Hinton, J. C. D., and Richardson, D. J. (2008) A combination of cytochrome c nitrite reductase (NrfA) and flavorubredoxin (NorV) protects *Salmonella enterica* serovar Typhimurium against killing by NO in anoxic environments. *Microbiology 154*, 1218−1228.

(7) Le Fourn, C., Brasseur, G., Brochier-Armanet, C., Pieulle, L., Brioukhanov, A., Ollivier, B., and Dolla, A. (2011) An oxygen reduction chain in the hyperthermophilic anaerobe *Thermotoga maritima* highlights horizontal gene transfer between *Thermococcales* and *Thermotogales*. *Environ. Microbiol. 13*, 2132−2145.

(8) Thorgersen, M. P., Stirrett, K., Scott, R. A., and Adams, M. W. W. (2012) Mechanism of oxygen detoxification by the surprisingly oxygen-tolerant hyperthermophilic archaeon, *Pyrococcus furiosus*. *Proc. Natl. Acad. Sci. U.S.A. 109*, 18547−18552.

(9) Kern, M., Volz, J., and Simon, J. (2011) The oxidative and nitrosative stress defence network of *Wolinella succinogenes*: Cytochrome c nitrite reductase mediates the stress response to nitrite, nitric oxide, hydroxylamine and hydrogen peroxide. *Environ. Microbiol. 13*, 2478−2494.

(10) Hillmann, F., Riebe, O., Fischer, R. J., Mot, A., Caranto, J. D., Kurtz, D. M., Jr., and Bahl, H. (2009) Reductive dioxygen scavenging by flavo-diiron proteins of *Clostridium acetobutylicum*. *FEBS Lett. 583*, 241−245.

(11) Hayashi, T., Caranto, J. D., Wampler, D. A., Kurtz, D. M., Jr., and Moenne-Loccoz, P. (2010) Insights into the nitric oxide reductase mechanism of flavodiiron proteins from a flavin-free enzyme. *Biochemistry 49*, 7040−7049.

(12) Fang, H., Caranto, J. D., Mendoza, R., Taylor, A. B., Hart, P. J., and Kurtz, D. M., Jr. (2012) Histidine ligand variants of a flavo-diiron protein: Effects on structure and activities. *JBIC, J. Biol. Inorg. Chem. 17*, 1231−1239.

(13) Enemark, J. H., and Feltham, R. D. (1974) Principles of structure, bonding, and reactivity for metal nitrosyl complexes. *Coord. Chem. Rev. 13*, 339−406.

(14) Nocek, J. M., Kurtz, D. M., Jr., Sage, J. T., Xia, Y. M., Debrunner, P., Shiemke, A. K., Sanders-Loehr, J., and Loehr, T. M. (1988) Nitric oxide adducts of the binuclear iron site of hemerythrin: Spectroscopy and reactivity. *Biochemistry 27*, 1014−1024.

(15) Rodriguez, J. H., Xia, Y.-M., and Debrunner, P. G. (1999) Mössbauer spectroscopy of the spin coupled Fe^{2+}-$\{FeNO\}^7$ centers of nitrosyl derivatives of deoxy hemerythrin and density functional theory of the $\{FeNO\}^7$ motif. *J. Am. Chem. Soc. 121*, 7846−7863.

(16) Hayashi, T., Caranto, J. D., Matsumura, H., Kurtz, D. M., Jr., and Moënne-Loccoz, P. J. (2012) Vibrational analysis of mononitrosyl complexes in hemerythrin and flavodiiron proteins: Relevance to detoxifying NO reductase. *J. Am. Chem. Soc. 134*, 6878−6884.

(17) Caranto, J. D., Weitz, A., Hendrich, M. P., and Kurtz, D. M., Jr. (2014) The nitric oxide reductase mechanism of a flavo-diiron protein: Identification of active-site intermediates and products. *J. Am. Chem. Soc. 136*, 7981−7992.

(18) Arciero, D. M., Lipscomb, J. D., Huynh, B. H., Kent, T. A., and Munck, E. (1983) EPR and Mössbauer studies of protocatechuate 4,5-dioxygenase. Characterization of a new Fe^{2+} environment. *J. Biol. Chem. 258*, 4981−4991.

(19) Di Matteo, A., Scandurra, F. M., Testa, F., Forte, E., Sarti, P., Brunori, M., and Giuffre, A. (2008) The O_2-scavenging flavodiiron protein in the human parasite *Giardia intestinalis*. *J. Biol. Chem. 283*, 4061−4068.